OPEN LOOP CONTROL SYSTEM AND TOOLS FOR DATA ACQUISITION AND ESTIMATION OF THE WELD BEAD DEPTH IN GMAW PROCESS

Guillermo A. Bestard*, Renato C. Sampaio†, Sadek C. A. Alfaro‡

*Electronic Engineering Group, Faculty of Gama, University of Brasília
Área Especial de Indústria Projeção A, Gama, DF, Brazil

†Software Engineering Group, Faculty of Gama, University of Brasília
Área Especial de Indústria Projeção A, Gama, DF, Brazil

‡Department of Mechanical and Mechatronic Engineering, Faculty of Technology
University of Brasília, Campus Darcy Ribeiro, Brasília, DF, Brazil

Emails: guillermo@unb.br, renatocoral@unb.br, sadek@unb.br

Abstract— Gas Metal Arc Welding process is extensively used in many industries. The geometry of weld bead is very important and commonly used for quality validation, but an on-line measurement is challenging due to the extreme environmental conditions on the welding arc. These conditions limit the process automation since the control loop cannot be closed with classical instrumentation techniques. The system developed in this work, collects arc welding variables, depth of the weld bead and thermographic information of the molten weld pool. It integrated non-contact sensors with image processing algorithms and allow the real-time control in open loop. A novel algorithm for obtaining a dynamic model to estimate the depth of the weld bead was developed, based on these techniques. The estimators use a multilayer perceptron neural network and are optimized for embedded devices and real-time processing on a Field-Programmable Gate Array device. The results show that the system and proposed method is useful in industrial and research environments.

Keywords— data acquisition, image processing, infrared thermography, weld bead depth

Resumo— O processo de soldagem GMAW é amplamente utilizado na indústria. A geometria do cordão de solda é importante e comumente usada para validação de qualidade, mas uma medição on-line é desafiadora devido às condições ambientais extremas no arco elétrico. Essas condições limitam a automação do processo, pois a malha de controle não pode ser fechada com técnicas de instrumentação convencionáis. O sistema desenvolvido neste trabalho, coleta as varaiveis do arco, a profundidade do cordão de solda e as informações termográficas da poça de fusão. Integra sensores sem contato com algoritmos de processamento de imagem e permite o controle em tempo real do processo em malha aberta. Um novo algoritmo para obter modelos dinâmicos do process e estimar a penetração do cordão de solda, foi desenvolvido com base nessas técnicas. Os estimadores usam uma rede neural perceptron multicamada e são otimizados para dispositivos embarcados e processamento em tempo real em um dispositivo FPGA. Os resultados mostram que o sistema e o método proposto são úteis em ambientes industriais e de pesquisa

Palavras-chave— adquisição de dados, penetração do cordão de solda, procesamento de imagen, termografía infravermelha

1 Introduction

Gas Metal Arc Welding (GMAW) process is versatile and allows for high-quality weld beads. Although its extensive industrial application, the use of the automatic form is limited by the extreme environmental conditions imposed for the welding arc. The control of the weld bead geometry is very important for obtaining good results in this process and is commonly used for quality validation, but an on-line measurement is very difficult in these conditions. Weld bead geometry includes width, reinforcement and depth, which are shown in Figure 1. These geometry parameters are governed by many factors, such as welding current, welding voltage, wire feed speed, welding speed and the contact tip to work distance (Kielhorn et al., 2002)

Infrared thermography provides a non-contact measurement of the molten weld pool temperature. Infrared sensing of arc welding processes has been extensively investigated and the information provided by this measurement technique can help to determinate the weld bead depth (Chen et al., 1988; Nagarajan et al., 1989; Nagarajan et al., 1990; S. Nagarajan et al., 1992; Beardsley et al., 1994; Chokkalingham et al., 2012) and welding quality (Alfaro, 2012; Sreedhar et al., 2012; Alfaro et al., 2015). Since 1971 several patents have been registered on the use of infrared emission information to total penetration detection and control (Iceland and Martin E. O'Dor, 1971; Bangs et al., 1989).

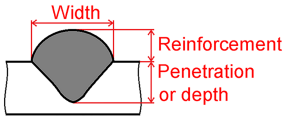

Figure 1: Geometric parameters of the weld bead

This paper presents a system developed to send a stimulus to the welding process and to collect values of the arc variables, infrared thermography and weld bead depth. The system allows real-time open loop process control. Algorithms were developed to extract features of ther-

mographic data and depth of the weld bead on macrographic images. It is used for research in doctoral projects. The actual application area is the automatic control, arc welding and sensor fusion research.

2 Data acquisition and open loop control system for GMAW welding process

The data acquisition and open loop control system has five main components: a welding power source, a welding table, data acquisition and control interfaces, a thermographic camera and a computer where a data acquisition and data processing software are run. The interface and software were developed for this application. The components and data flow are shown in Figure 2 and are described in the next sections.

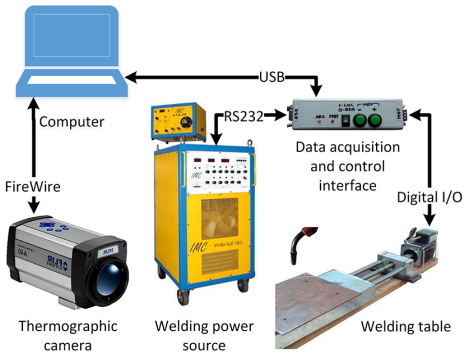

Figure 2: Components of the data acquisition and open loop control system

2.1 *Flat welding table*

The flat welding table is an electro-mechanical system development by GRACO students (Franco, 2008). It is integrated by a linear axis that provides a step of 5 mm by revolution and a stepper motor of 1.8 grades by step.

The stepper motor is controlled by a driver circuit with signals for modifying the stepper time (speed) and direction. Other signals show the status of the driver and protect against overload. This structure supports 15 Kg of load and 15 mm/s of maximum speed. This system is used to move the piece, keeping the welding torch fixed. It is shown in Figure 3.

2.2 *Welding power source*

The welding power source is the Inversal 450 (IMC-Soldagem, 2005). The communication algorithm for remote control and data acquisition was developed, based on RS232 communication protocol. A state machine, implemented in the control interface (see section 2.3), defines the operation parameters and obtains the measurements and status of the welding power source. The operation sequence for controlling the welding power source and the data acquisition software was also developed. This sequence uses a state machine

Figure 3: Flat welding table and instruments support

and it is repeated continuously into the main program. It is shown in Figure 4a.

The sequence is started only if the RS232 transmission buffer is empty. When the interface sends a command, a timer is activated. If the timer value is greater than the maximum response time, the "time out" flag is activated and the program execution exits the sequence. In the next cycle, if the "time out" flag is true, the synchronization command is sent to the welding power source and the communication is restored.

There are two blocks in the sequence: configuration and arc open state sequence. To increase the data acquisition speed, the configuration parameters are sent to the welding power source only when the arc is closed. The necessary commands for process control are always executed, including the open and close arc sequence when necessary. When the arc is closed, the wire feed direction is inverted and the wire feed speed is increased by a few milliseconds. This rollback wire prevents the trapping of the wire in the welding bead. Finally, in each cycle, the arc status is read and the cycle time is updated. In this algorithm, the measurement unit conversion, the numerical formats conversion and the treatment of communication errors are required.

2.3 *Data acquisition and open loop control interface*

The data acquisition and control interface synchronizes the piece movement with the welding power source operation and obtains the process measurements in real-time. The interface is connected to the welding power source through an RS232 port, to a computer through a USB port and to the driver circuit of the stepper motor by digital signals, as is shown in Figure 2.

Figure 5 shows the interface, where the manual controls to move the welding table such as the remote or manual operation selector, the *Motor On* and *Open Arc* indicators, and the external connections can be observed. A small piezoelec-

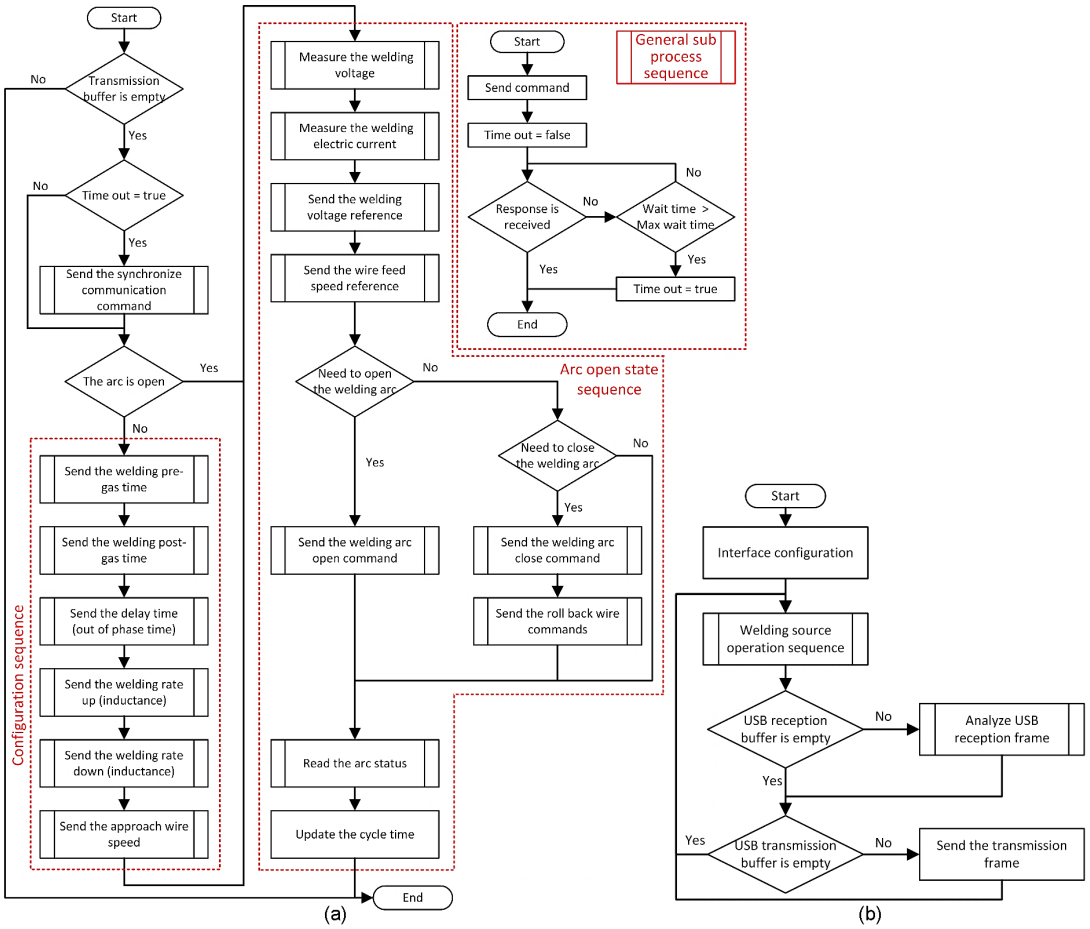

Figure 4: Block diagram of operation sequence: (a) Welding power source communication sequence; (b) Main loop sequence of the interface

tric horn emits sounds indicating the start or the end of welding sequence or if an error occurs. The simplicity of the hardware, small size and low cost of its components, make this interface accessible for low budget projects.

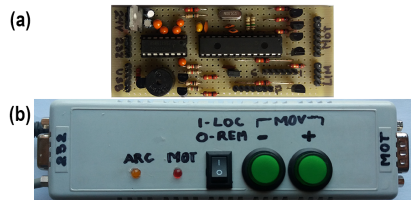

Figure 5: Data acquisition and control interface: (a) Internal circuit; (b) External view

The electronic circuit is shown in Figure 6. The interface needs a power supply between 7 V and 24 V, which is connected to P1. The USB and RS232 communication wires are connected to P2 and P5 respectively. The motor driver connects to P6. P3 gets the state of the pushbutton and switch, and drivers the light indicators in the panel. P7 is used for the limit detector of the welding table while P4 is the interface to program the microcontroller.

The operation is controlled by a PIC18F2550 microcontroller . Before starting the welding, the microcontroller receives from the computer, the sequence of values to be sent to the welding power source in each position of the piece. These values are fixed by the user in the data acquisition program (see section 2.5). The start and end point of the weld, the welding speed and the sampling period or the distance between samples are defined by the user according to the selected work mode.

Following that, the interface has an autonomous and independent operation and sends the measurements obtained of position to a computer in real-time . The acquisition program obtains the thermographic data regardless of the clock or priorities of the operating system. The main loop of the firmware is drawn in Figure 4b.

The development of the interface requires a detailed study of the welding power source communication protocol and numerous tests. To monitor and control the operation of the welding power source a state machine was used to minimize the communication time and ensure an acceptable sampling period (see section 2.3)

The communication protocol between the interface and the computer was created based on ASCII characters. This allows the full control of the welding power source, the welding table, the interface and the operation sequence of the process. The interface controls the driver circuit of the stepper motor and verifies the occurrence of

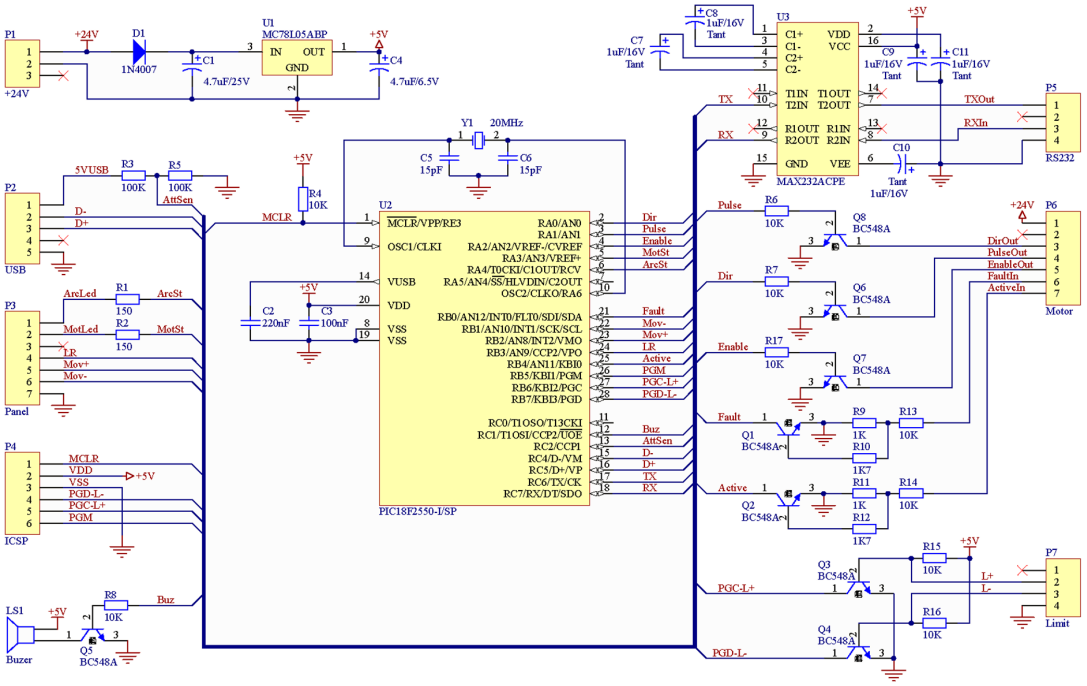

Figure 6: Schematic of the electronic circuit of the data acquisition and control interface

an error by the feedback signal. The processing of these signals is done by timer interruptions, which are adjusted by the step time.

Two modes of operation are available for data acquisition. One is based on a sampling time and is controlled by a timer interruption between 5 and 500 ms. In this mode, in each interruption, a data set is sent to the computer. It has the disadvantage that by varying the speed of movement the distance between samples will vary.

The other mode is based on comparing the position increment with a steep value preset by the user. Once this increment is equal to the preset value, a new data set is sent to the computer. This is repeated in equal intervals of position, independently of the movement speed and provides equidistant measurements in the piece.

2.4 Thermographic camera

The ThermoVision A40 thermographic camera (FLIR-Systems, 2004) is used for obtaining the temperature values from the molten puddle. It employs a semiconductor sensor of focal plane array uncooled microbolometer technology. It has a spectral range between 7.5 and 13 μm, a temperature range between -40°C and 2000°C, a sampling frequency of 120 Hz (120 fps) and a maximum resolution of 16-bit monochrome and 8-bit color. The data is obtained from a Firewire interface in a matrix format, with the temperature of each pixel of the image. Among other notable features, it has an automatic correction of the measurement by the effects of environmental reflection, temperature, distance, relative humidity and external optics that could have coupled.

2.5 Data acquisition and stimulus sequence design software

ThermoDataWelding (TDW) was developed in Visual Studio using libraries provided by the thermographic camera manufacturer (FLIR-Systems, 2004). This program collects and stores the data of the welding process and the operation of the whole system in text files. The status bar continuously displays the status of the communication with the data acquisition interface, the welding power source and the thermographic camera. The main form is shown in Figure 7.

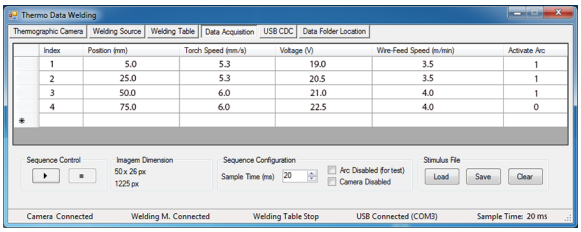

Figure 7: Data acquisition and stimulus sequence design module

The TDW is divided into six modules oriented to specific functions that are discussed below:

Thermographic Camera: It allows the configuration and verification of the camera. It shows the thermographic image, the maximum and minimum values, and a profile of the line that contains the maximum value.

Welding Power Source: It sets the fixed welding parameters. This includes the inductance, pregas and post-gas times, gap wire-arc time, wire diameter, contact tip to work distance, type and thickness of material, composition and flow rate of shielding gas.

Welding Table: It facilitates the adjustment of the piece's initial position in the welding table and shows the state of the control interface.

Data Acquisition: It provides a tool to create the welding sequence. This includes the start and end positions, the stimulus to send to the welding power source and the sampling period. The user starts the process and it stops automatically when the sequence ends, or when is stopped manually. Three files are created in each experiment that store the system configuration, the stimulus sequence and the measurements collected.

USB CDC: Sets the communication port where the data acquisition interface is connected.

Data Folder Location: Defines the folder where the configuration and measurements files are stored.

2.6 *Feature extraction of the infrared image*

The infrared matrix (supplied by the camera) is processed with the feature extraction algorithm to obtain, in each sampling period, the thermographic peak, the base plane, the curve width, the area and the volume parameters. This information is used to analyze the weld bead geometry. An example of the algorithm output is shown in Figure 8.

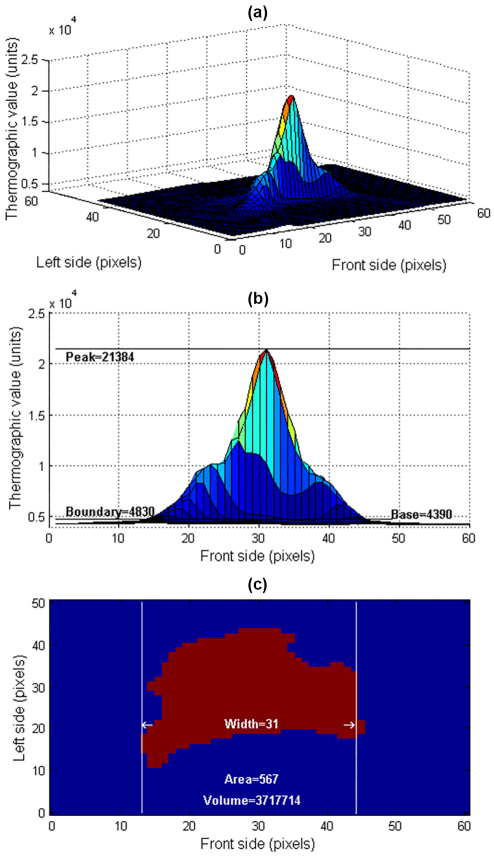

Figure 8: Features extracted from the infrared image of a sample data: (a) Thermographic 3D view; (b) Front view; (c) Boundary plane (blue) and detected area (red)

The data processing algorithm includes a moving average filter of 3x3 pixels and statistical analysis. The thermographic peak or maximum value of the matrix is calculated. The base plane is calculated as the average of 10% of the values in the left and right edges (left and right side, see Figure 8b). The boundary plane is 10% above the base plane.

The intersection plane between the thermographic surface and the boundary plane is the area and the maximum width in the front axis is the width (see Figure 8c). The sum of the thermographic values within the intersection plane is the thermographic volume.

2.7 *Image processing for offline measuring of the weld bead depth*

The weld bead depth profile can be obtained from the macrographic analysis. To this end, a cut is made in the longitudinal direction (i.e., in the direction of the torch movement). If a bad alignment of the cut tool with the weld bead occurs, a new cut is necessary. In these cases, we take the maximum value in each measurement point.

In the processing, the specimen will be polished and etched using a 2.5% Nital solution to display the weld bead penetration. In a similar position that is shown in Figure 9, a picture will be taken and analyzed with image processing algorithms.

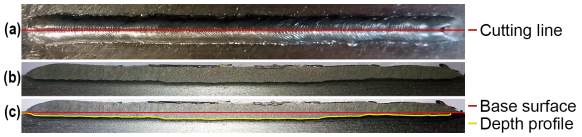

Figure 9: Weld bead depth obtained using image processing algorithms: (a) Longitudinal cut of the weld bead; (b) Polished piece; (c) Bead depth profile and the base surface

The algorithm, developed in Matlab, corrects image misalignment and filters the image for a border detection procedure. The baseline (shown in red in Figure 9) is detected. The piece thickness and length is known and used to calculate the scale coefficients. The weld bead penetration limit is detected (shown in yellow) and the difference between it and the base line returns as the weld bead depth profile. The profile is filtered and the missing values are repaired with the interpolation method.

2.8 *Sensor fusion to estimate the depth of the weld bead*

A cooperative, data-in/data-out and centralized sensor fusion (Bestard and Alfaro, 2015) algorithm was developed in (Bestard, 2017), based on a Multilayer Perceptron (MLP) artificial neural network to estimate the depth of the weld bead. The inputs of the neural network add previous measurements and estimates values to capture the process dynamics.

The MLP has eight neurons in the input layer, twelve in the hidden layers and one in the output layer, that gives the weld bead depth ($\hat{D}$). The input variables are the thermographic peak (Tp), the thermographic base (Tb), the thermographic area (Ta), the thermographic volume (Tv), the thermographic width (Tw), the measurements of welding current (i) in the actual (nT) and previous sample (nT-T) and the previous estimated value ($\hat{D}(nT\text{-}T)$). The symbol T is the sample time and n is the sample number. The activate function is the hyperbolic tangent sigmoid transfer function. Figure 10 shows the block diagram of the estimator.

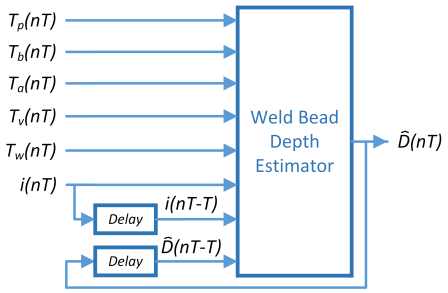

Figure 10: The estimator of weld bead depth that uses the thermographic features with welding current in cooperative mode

The network training should be done with experimental measurements of the parameters of input and output, obtained from the data acquisition system and infrared feature extraction techniques, and by using the backpropagation algorithm. The real values of the weld bead depth are obtained from the macrographic analysis. For a better training performance, all inputs have to be normalized in the interval [-1,1]. This dynamic estimator model is valid only for the current process conditions and must be updated if these change.

We must emphasize the importance of simplifying the estimating algorithm due to real-time requirements. The use of the proposed parameters and not the complete infrared image can help reduce the resources used and increase the speed of the estimation process.

The MLP implementation in FPGA consists of multiple neurons in parallel, which are synchronized and controlled by a Finite State Machine (FSM) as shown in (Bestard et al., 2017). All operations are carried out using customized variable width floating-point arithmetic and trigonometric libraries based on the IEEE 754 standard. The MLP architecture was optimized to reduce the resources in FPGA device.

3 Results and Discussion

Four welding experiments were made using carbon steel pieces with dimensions of 85x50x6mm on which welds were laid adopting the bead-on-plate technique (welding on top) in a horizontal position. The pieces surfaces were cleaned to eliminate any dirt and oxides. The torch was fixed at 90° from the horizontal plane and 12 mm of contact tip to work distance. The shielding gas was composed of 98% Argon and 2% Oxygen, with 15 psi of pressure. Steel welding electrode with a diameter of 1 mm (Product code CA-JMERS6100S015W00 of Merit®S-6 Lincoln Electric) was used. The welding power source was configured (through the interface) with a rate up and a rate down of 50, 2 s of pre-gas time, 1.5 s of post-gas time and 0.05 s of gap time. The sampling time was 20 ms. The dimensions of the thermographic image were 49x25 pixels.

One of the four experiments is presented in this paper. In this experiment, the welding voltage is constant. The welding speed and wire feed speed received a growing stimulus at 30 s and a decreasing stimulus at 60 s, keeping a constant relation. The table on Figure 7 shows this sequence and Figure 11 shows the measurements obtained using the system described in the previous sections.

The correlation between the wire feed speed and the welding current is observed in Figure 11. When the wire feed speed is increased the welding current increases too.

Also, it is possible to notice that although the wire feed speed is changed, the bead width and the bead reinforcement remain stable because of the constant relationship between wire feed speed and welding speed and the constant value of the welding voltage.

The autocorrelation and cross-correlation coefficients show high values, indicating a satisfactory sampling time and a delay of 11 sampling times between the weld bead depth and the stimulus.

The system validation shows a good behavior in real-time with acceptable accuracy and performance. The data collected and the model obtained are examples of the usefulness of the system for research activities that do not have many resources and equipment.

The model has a fit of 0.99844, a performance or median square error (MSE) of $7.61\text{x}10^{-4}$ at epoch 6, a closed-loop performance of $6.4\text{x}10^{-3}$ and the network response is very good. The model test with a different experimental data set had a fit of 0.9901 and the performance was $8.076\text{x}10^{-4}$. The closed-loop performance was 0.244 and the network response was very good with an estimation error of less than 0.1 mm. The response curves in Figure 12b, show that the model is able to reproduce the behavior of the process with accuracy. The calculation of estimation error is low (less than 0.05mm or less than 5% of full range) in all the curve.

The MLP was synthesized using Intel® Quartus® Prime 15.1 (from Altera Corp.) for

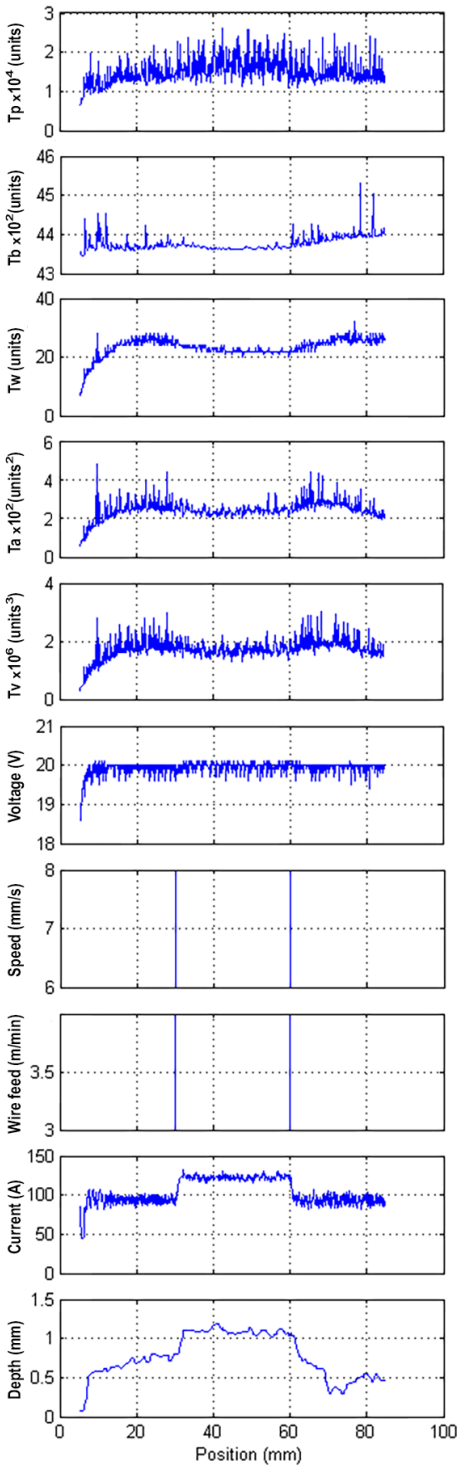

Figure 11: Experimental measurements obtained with the data acquisition and control system. Adapted from (Bestard, 2017)

the target FPGA (Cyclone V-5CSEMA5F31C6N) kit DE1-SoC from Terasic Inc. The architecture was simulated using Mentor Graphics QuestaSim 10.6c from Mentor Graphics Corp. The floating-point (FP) units have configurable precision and experiments were conducted using FP units (32, 27, 24 and 18 bits). The exponent width was fixed (8 bits) and the mantissa had variable sizes.

Simulation results are shown in Figure 12c. The hardware simulation output is compared to experimental data measurements and shows satisfactory performance for all architectures. The one using 18-bits floating point precision as can be noticed by the noisy red dotted signal. The chosen architecture was 24 bits of precision which can run at 130 MHz and compute the output in 1.54 us. The MSE for this architecture was 2.094×10^{-4}.

4 Conclusions

A low-cost data acquisition and open-loop control system was developed based on a microcontroller device. It sends stimulus and captures the dynamics of the welding process to model the geometry of the weld bead. The results showed a good performance of the system.

The image processing techniques, developed to obtain the depth of the weld bead over its entire length, offer satisfactory results without using a complex optical equipment.

The sensor fusion algorithm to estimate the weld bead depth, using the arc variables and the thermographic information collected by the system, showed satisfactory accuracy and good real-time performance in the FPGA implementation.

This system is used to research in the Automation and Control Group in Manufacturing Processes (GRACO) of Brasilia University and can also be used in industrial conditions.

5 Acknowledgments

This work has been supported by the University of Brasilia (UnB), the government research CAPES foundation and CNPq. In the development of the communication algorithm and the operation sequence of the welding power source, the authors received an invaluable support from Professor Ph.D Raul Gohr Jr, of the IMC-Soldagem company.

References

Alfaro, S. C. A. (2012). Sensors for quality control in welding, *Soldagem & Inspeção* **17**(3): 192–200.

Alfaro, S. C. A., Vargas, J. A. R., Carvalho, G. C. D. and de Souza, G. G. (2015). Characterization of Humping in the GTA welding process using infrared images, *Journal of Materials Processing Technology* **223**: 216–224.

Bangs, E. R., Longinow, N. E. and Blaha, J. R. (1989). Using infrared image to monitor and control welding, http://illinois.patentlibrary.us/us-4877940.html.

Beardsley, H., Zhang, Y. M. and Kovacevic, R. (1994). Infrared sensing of full penetration state in gas tungsten arc welding, *International Journal of Machine Tool and Manufacturing* **34**(8): 1079–1090.

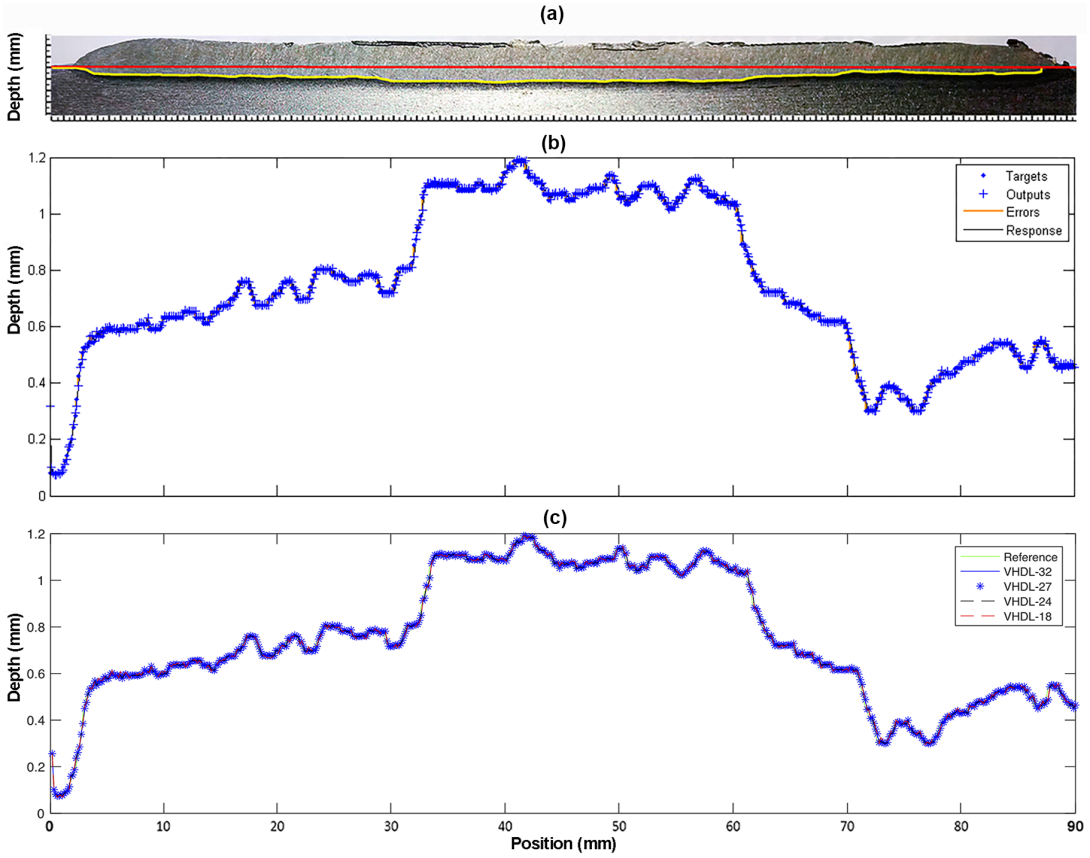

Figure 12: Measurements and simulations results: (a) Experimental measurements of the weld bead depth; (b) MLP simulation; (c) Hardware simulation. Adapted from (Bestard, 2017)

Bestard, G. A. (2017). *Sensor fusion and embedded devices to estimate and control the depth and width of the weld bead in real time*, PhD thesis, Universidade de Brasília.

Bestard, G. A. and Alfaro, S. C. A. (2015). Sensor fusion: theory review and applications, *23rd ABCM International Congress of Mechanical Engineering COBEM 2015*, Rio de Janeiro, Brazil.

Bestard, G. A., Sampaio, R. C., Vargas, J. A. R. and Alfaro, S. C. A. (2017). Sensor Fusion to Estimate the Depth and Width of the Weld Bead in Real Time in GMAW Processes, *Sensors (Basel, Switzerland)* **18**(962): 151.

Chen, W. H., Nagarajan, S. and Chin, B. A. (1988). Weld penetration sensing and control, *Infrared Technology* **972**(XIV): 268–272.

Chokkalingham, S., Chandrasekhar, N. and Vasudevan, M. (2012). Predicting the depth of penetration and weld bead width from the infra red thermal image of the weld pool using artificial neural network modeling, *Journal of Intelligent Manufacturing* **23**(5): 1995–2001.

FLIR-Systems (2004). ThermoVision A40 M Manual del usuario, *Technical report*, FLIR Systems.

Franco, F. D. (2008). *Monitorização e localização de defeitos na soldagem TIG através do sensoriamento infravermelho. Master Thesis*, Master thesis, Universidad de Brasília.

Iceland, W. F. and Martin E. O'Dor (1971). Weld penetration control.

IMC-Soldagem (2005). Manual de Instruções Inversal 450/600, https://www.imc-soldagem.com.br.

Kielhorn, W. H., Adonyi, Y., Holdren, R. L., Horrocks, R. C. and Nissley, N. E. (2002). *Survey of Joining, Cutting and Allied Processes*, American Welding Society.

Nagarajan, S., Banerjee, P., Chen, W. and Chin, B. A. (1990). Weld pool size and position control using IR sensors, *Proceedings of NSF Design and Manufacturing Systems Conference*, Arizona State University.

Nagarajan, S., Chen H., W. and Chin, B. A. (1989). Infrared sensing for adaptive arc welding, *Welding Journal* **68**(11): 462–466.

S. Nagarajan, Chin, B. and Chen., W. (1992). Control of the welding process using infrared sensors, *IEEE Transactions on Robotics and Automation* **8**(1): 86–93.

Sreedhar, U., Krishnamurthy, C. V., Balasubramaniam, K., Raghupathy, V. D. and Ravisankar, S. (2012). Automatic defect identification using thermal image analysis for online weld quality monitoring, *Journal of Materials Processing Tech.* **212**(7): 1557–1566.